Microstructural and current-voltage characteristics in $Mo/HfO_2/n$-Si based metal-insulator-semiconductor (MIS) Schottky diodes using different methods

V. Manjunath[1]*, S Dastagiri[2], M. Vani[3], G. Nagaraju[4], M. V. Lakshmaiah[2*]

[1]Department of Physics, Sri Padmavati Mahila Viswavidyalayam, Tirupati, A.P., India
[2]Department of Physics, Sri Krishnadevaraya University, A.P, India-515003.
[3]Department of Physics (Electronics), Sri Venkateswara University, Tirupati, A.P, India-517 502
[4]Department of Applied Micro biology,Sri Padmavati Mahila Visvavidyalayam, A.P, India-517 502

E-mail address: drvmanju18@gmail.com (***Dr. V. Manjunath***)*Corresponding author.

E-mail address:drmvl2009@gmail.com (Dr. ***M.V.Lakshmaiah***) *Co-Corresponding author.

ABSTRACT

This paper investigates the effect of hafnium dioxide (HfO_2) thin film as interlayer between the Mo and n-Si semiconductor on the electrical characteristics of the Mo/n-SiSchottkydiode (SD). The X-ray photoelectron spectroscopy (XPS) and X-ray diffraction (XRD)results confirmed that HfO_2films were formed on the n-Si semiconductors.The image from SEM displays that the deposited HfO_2 thin film had a uniform appearance good smoothness of the surface. The smooth surfaces of the insulating layer strongly influence the electrical properties of the diode.The electrical properties of the $Mo/HfO_2/n$-Si metal/insulator/semiconductor (MIS) diode were obtained via current-voltage (I-V) measurements in the voltage range from −3 V to +3 V at room temperature. The MIS diode displayed a superior rectifying nature and a lower reverse leakage current. The barrier height (Φ_b) and ideality factor value of the MIS dide was estimated to be 0.85 eV and 1.21. A higher Φ_b was attained for the MIS diode which enabled the HfO_2interlayer to alter Φ_b. The Φ_b values are derived from the I-V, Hernandez, Cheung, and Norde methods and the derived values were comparable to one another, which indicate their consistency and validity. The forward bias log (I) - log (V) curve of the MIS diode revealed the ohmic nature in low-voltage regimes and space-charge-limited conduction in high-voltage regimes. However, for the MIS diode, the Poole-Frenkel and Schottky emissions are the dominant current

conduction mechanisms in the lower and higher bias regions.These outcomes indicate that the HfO_2film can be chosen as dielectric materials in the construction of MIS devices.

Keywords: High-k HfO_2, n-type Si, MIS diode, structural and electrical properties.

1. Introduction:

Schottky diode (SDs) is such a helpful component since it can be utilised as a switch in radio frequency applications and as a rectifier in power applications. Studies on the characteristics and uses of these devices have been extensively studied [1-7]. In these SDs, it is important to understand the nature of the transmission mechanism and interface homogeneity [3]. Among the most crucial factors affecting the physical and electrical properties of Schottky diode devices are the preparation conditions and the interfacial layer's fabrication processes. The existence of an interface layer between the upper contact and the semiconductor can be motive to change some features of diodes [8].

Various metal oxides such as SiO_2, V_2O_5, Ga_2O_3,TaO_2, TiO_2, ZrO_2, Ta_2O_5, Sm_2O_3, Al_2O_3 and HfO_2 [9-13] have been used as an interfacial layer for SDs. Among them, HfO_2 plays an important role in SDs. HfO_2 has attracted attention due to its chemical and good thermal stability [13], high dielectric constant (~25) [14], high refractive index and large band gap width (5.4 eV) and infrared bands and good transmittance in ultraviolet, making it a competitive candidate for Schottky diode diodes, optical materials and resistive switching oxides [15–17]. Controlling the characteristics of the interlayer is therefore critical for improving the device performance level. For example, Al/HfO_2/p-Si (MIS) structures were created by Ozden et al. using the sol-gel process at three different annealing temperatures and insulating layer thicknesses. They demonstrated that as insulator layer thickness is increased, ideality factor (n) and interface state density (Nss) values increase [18]. Al/HfO_2/n-Si (SDs) were developed by Harishsenthil et al. using various HfO_2 substrate temperatures. They suggested that the substrate temperatures had a significant impact on the diode characteristics

[19]. By depositing ALD, Kaufmann et al. developed the insulating layers of HfO_2 and TiO_2 with thicknesses of 1, 2, and 4 nm. By adjusting the measurement temperature (297-373 K), current-voltage curves were derived from the diodes. For both dielectrics, thicker insulating layers result in larger n and lower SBH real values [20]. The hydrogen detection capabilities of a Pd/HfO_2/GaN-based MOS structure at varied hydrogen gas concentrations are studied by Chen et al. [15]. When exposed to 1% H_2/air gas at 300 K, the examined MOS structure displays a good hydrogen detecting response of 4.9×10^5 (139) under an applied forward- (reverse-) voltage of 0.5 V (-2 V).The Pt/HfO_2/n-GaN MIS structure underwent I-V characterization throughout a temperature range of 150 K to 370 K by Shetty et al. [12] in order to better understand the Pt/HfO_2/GaN interface. The BH increased (from 0.3 eV to 0.79 eV) and the ideality factor decreased (from 3.6 to 1.2) as the temperature increased from 150 K to 370 K.Both theoretical and practical researches have proven that the interface layer in MS devices has a considerable impact on the dielectric characteristics and other fundamental electrical parameters. Studying the electrical parameters that affect the effectiveness, stability, and dependability of the device is crucial.

Despite the potential benefits of HfO_2 thin films as a high-dielectric-index oxide interlayer, there are some research reports on the fabrication and electrical characterization of HfO_2/Si diodes using various metal contacts. To the best of our knowledge, no studies on the fabrication and characterization of molybdenum (Mo) as a Schottky electrode, aluminium (Al) as an ohmic contact, and HfO_2 as an insulating layer on n-type Silicon (Si) substrate to prepare MIS SDs have been published.In order to do this, radio frequency (RF) and direct current (DC) magnetron sputtering were used to fabricate the Mo/HfO_2/n-Si metal-insulator-semiconductor (MIS) type Schottky diode. The MIS diode, microstructural, morphological and electrical characteristics are therefore prepared and characterised.First, the microstructural and morpological characteristics of the HfO_2 film on the Si substrate are

examined using the well-known X-ray diffraction (XRD) and X-ray photoelectron spectroscopy (XPS) techniques.Second, the forward bias (FB) current-voltage (I-V) properties of MIS SD are investigatedat room temperature. The results have demonstrated that these types of structures are suitable for applications in optoelectronic devices.

2. Experimental Details

In this investigation, Si sample pieces measuring 1 cm by 1 cm were taken from an 8″ Si (100) wafer that had a thickness of 600 μm. An HfO_2 interlayer acts as an insulating layer to create n-Si-based SDs. Before deposition, the RAC method was applied to a regular, clean n-Si wafer with a resistivity of 1–10 Ω cm [40].Native oxides were eliminated using an $HF:H_2O$ (1:10) solution, which was followed by a deionized water rinse. Thermal evaporation was utilised to create an Al metallization with a 60 nm thickness on the rear (rough) side of the cleaned substrate (Si), which was then annealed in a quick thermal processing furnace at 300 °C for 10 minutes in N_2 gas to provide a suitable ohmic contact.Then, quartz glass and n-Si (smooth side) substrates were then coated with a thin layer of HfO_2 using RF-magnetron sputtering. Using a 50 mm diameter, 99.9% pure HfO_2 target, and argon as the sputter gas, four samples of HfO_2/Si diodes were fabricated.The target was pre-sputtered for 10 minutes in an Ar gas atmosphere to eliminate any surface contaminants. Finally, a top metal electrode made of Mo was deposited using direct current sputtering technology in a 1.2 mm 0.3 mm rectangular region with 70 W powers. The electrode has a thickness of 50 nm. The schematic representation of the Mo/HfO_2/Si SD is shown in Figure 1a. The microstructural, elemental, and morphological characteristics of the prepared HfO_2/Si device were analysed using the grazing index X-ray diffraction (GIXRD), X-ray photoelectron spectroscopy (XPS), and field emission scanning electron microscopy

(FESEM). A semiconductor analyzer (Keithley, Model-2636 semiconductor characterisation equipment) was used to conduct the I-V measurements at room temperature.

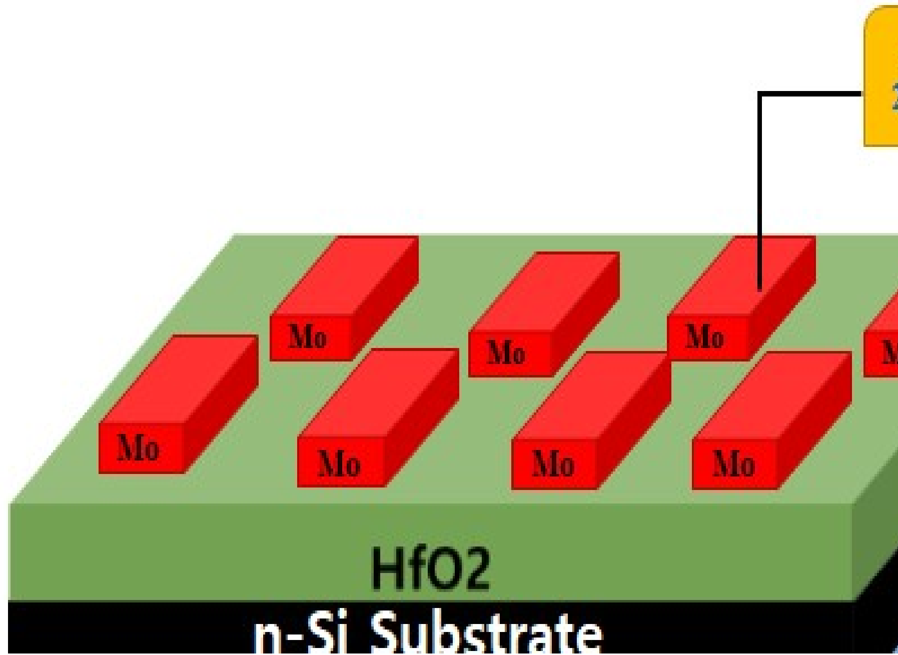

Fig. 1a. The schematic representation of the Mo/HfO_2/Si SD

3. Results and Discussions

The structural characteristics of HfO_2 film on n-Si were examined using XRD, as shown in Fig.1b. It was revealed that the existence of characteristic peaks of HfO_2 film. The characteristics peaks are observed at 17.47°, 24.42°, 28.25°, 31.65°, 34.53°, 38.80°, 45.21°, 50.72°, 56.24°, 60.64° and 66.02° for (100), (110), (002), (111), (020), (220), (211), (200), (130), (131) and (023), respectively. The HfO_2 thin film was subjected to XPS survey scans, and the typical wide survey HfO_2 thin film is shown in Fig.1b. The characteristic peaks ofHf (4f, 5p, 4d, 4p), O 1s, and O KLL (Auger peaks) are observed in the general survey spectra. Within the sensitivity of the equipment expecting the adsorbed ambient carbon, none of the contaminating species had been seen [21,22]. The image from SEM displays that the deposited HfO_2 thin filmhad a uniform appearance good smoothness of the surface.

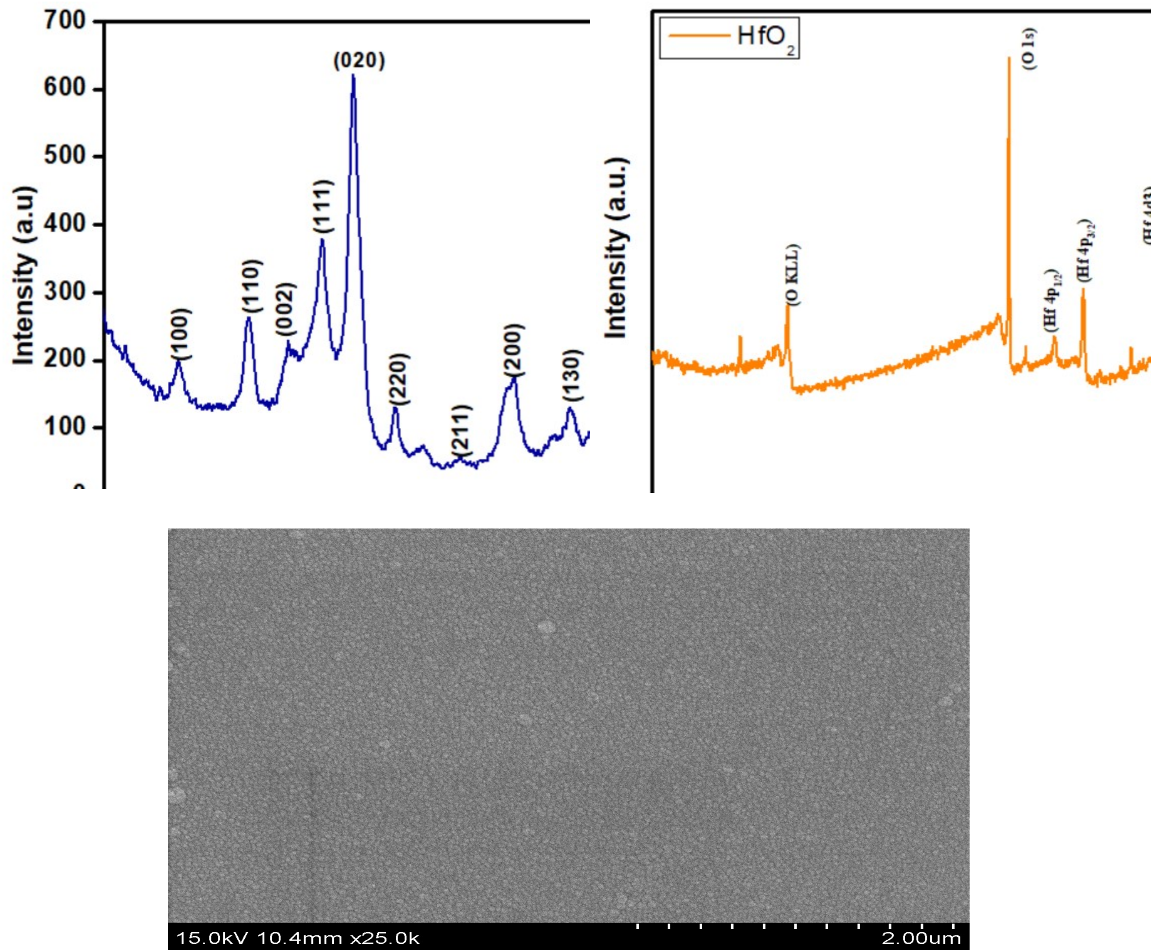

Fig.1b. XRD,XPS plots and SEM image of Mo/HfO_2/n-Si MIS SD

The HfO_2 interlayer is used in the fabrication of the Mo/HfO_2/n-Si MIS SD and evaluates their electrical properties. By using I-V measurements, the electrical characteristic of fabricated MIS SD is investigated. The experimental semi-logarithmic forward and reverse biased current-voltage (I-V) characteristics of Mo/HfO_2/n-Si MIS SD measured in the voltage range from -3V to +3V at room temperature presented in Fig. 2. Specifically, it is observed that the MIS diode shows low leakage current (1.53×10^{-6} A) at -1V. This implies that the HfO_2 as interlayer in between the metal and semiconductor influences the electrical properties of MIS diode. According to thermionic emission (TE) theory, the current through the Schottky barrier diode with the series resistance (R_S) and an interfacial layer at a forward bias (V>3kT/q), is given by the relation [23].

$$I = I_0 \exp\left[\frac{q(V-IR_S)}{nkT}\right]\left\{1-\exp\left[\frac{q(V-IR_S)}{kT}\right]\right\} \quad (1)$$

where V, IR_S, q, k, T, n, and I_0, A, A^*, and Φ_b have usual meanings [13, 14]. The reverse saturation current (I_0)is obtained from the intercept of the plot of ln I versus V at V = 0, given by

$$I_0 = AA^* T^2 \exp\left(-\frac{q\Phi_b}{kT}\right) \quad (2)$$

Once the saturation current I_0 has been determined, the Φ_b can be evaluated using the expression

$$\Phi_b = \frac{kT}{q}\ln\left(\frac{AA^*T^2}{I_0}\right) \quad (3)$$

The ideality factor (n) is measure of the conformity of the diode to pure TE, it is determined from the slope of the linear region of forward bias ln I-V using the relation

$$n = \frac{q}{kT}\left(\frac{dV}{d(\ln I)}\right) \quad (4)$$

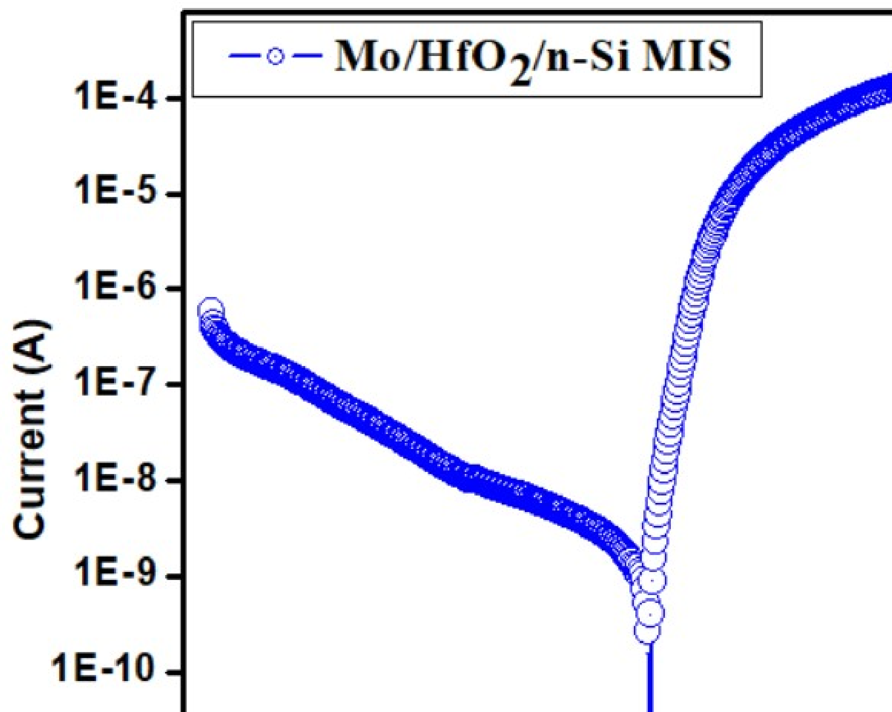

Fig. 2 Forward and reverse ln (*I*)–*V* characteristics of Mo/HfO_2/n-Si MIS SD measured at room temperature in the voltage range ± 3 V.

The Φ_b and n are measured to be 0.82eV and 1.21 for the SD. Due to an increase in the negative charges at the interface, analysis reveals that the higher barrier height. This might be caused by electron traps that are concentrated near the GaN interface [25]. Therefore, it is evident that the modified $\Phi_b$is likely the result of altered interfacial chemistry. The fact that the evaluated n MIS diode is greater than unity might be attributed to the different current transport processes, interfacial defects, and inhomogeneities in the interface [26]. For the higher n values, additional causes could include interface inhomogeneity, non-uniform interfacial charge distribution, the occurrence of surplus current, and recombination current caused by the interface states at the diode [27]. The deviation of the n from unity may be caused by the formation of an electric interlayer at the HfO_2/n-Si interface [28].

The R_S is significant in the non-linear curve region at the high applied voltage in the forward bias *I–V* characteristics. The main parameters such as '*n*' and R_S can also be evaluated by Cheung and Cheung method [29]. The Cheung's function can be written as

$$\frac{dV}{d(\ln I)} = \frac{nkT}{q} + IR_S \quad (5)$$

$$H(I) = V - \left(\frac{nkT}{q}\right)\ln\left(\frac{I}{AA^{**}T^2}\right) \quad (6)$$

H (I) is given as follows:

$$H(I) = n\Phi_b + IR_S \quad (7)$$

The d*V*/d(ln*I*) versus *I* curve for Mo/HfO_2/n-Si MIS SD is illustrated in Fig. 3. The plot should produce a straight line for the non-linear section of forward bias *I–V* characteristics. The 'R_S' and '*n*' values are calculated from slope and intercept of the plot as shown in Fig. 3. The extracted R_S and '*n*' values for Mo/HfO_2/n-Si MIS SD are 1000 Ω and 2.30, respectively. The *H* (*I*) versus *I* plot for Mo/HfO_2/n-Si MIS SD at 300 K is also shown in Fig. 3. According to Eq. (6), Fig. 3 also is a straight line with intercept (*y*-axis) equal to Φ_b results. The calculated $\Phi_b$and R_S values were 0.88 eV and 120 Ω, respectively. The R_S values acquired

from H (I) versus I plot are consistent with the dV/d(ln$I$) plot which signifies the reliability of the Cheung's methodology.

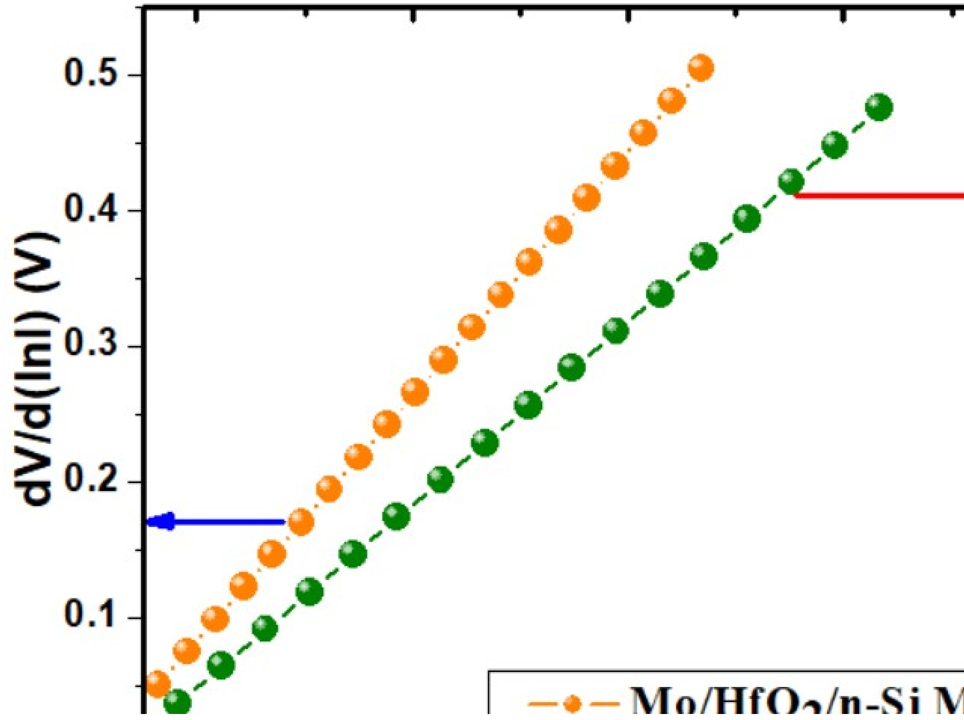

Fig. 3. Plot of dV/dln (I) and H (I) versus I for the Mo/HfO_2/n-Si MIS SD

In order to calculate the effective Φ_b of non-ideal SDs with little leakage current, Hernandez [30] suggested a novel approach. This approach is based on the idea that the Φ_b and n values are variables that depend on voltage. The expression for the voltage-dependent Z(V, T) functions is

$$Z\,(V,T)_i = \frac{kT}{q}\ln\left(\frac{I_i}{AA^{*}T^{2}[1-\exp(-qV_d/kT)]}\right) \quad (8)$$

$$Z(V,T)_i = -\Phi_b\,(V,T)_i + \frac{V_d}{n(V,T)_i} \quad (9)$$

where V_d is the diode voltage. The Z(V)-V_d plot is obtained from the linear region I-V characteristics using eq. (8). Fig. 4 shows the plot of $Z(V,T)_i$ versus V_d for the Mo/HfO_2/n-Si MIS diode. If $Z(V,T)_i$ varies linearly with V_d in the i-th voltage interval, then $\Phi_b(V,T)_i$ and $n(V,T)_i$ are constants and can be found from the slope and intercept, respectively. The values of $\Phi_b(V,T)_i$ and $n(V,T)_i$ have been found as 0.89 eV, 1.2 for MIS diode, respectively. It can be

seen that the values of the Φ_b and ideality factor obtained from the Z(V)-$V_d$plot and the conventional forward bias I-V method are similar to each other.To calculate consistent Φ_b and R_S values of Mo/HfO_2/n-Si MIS SD, an alternate method was developed by Norde and Bohlin [27, 28].Usually, the *n* values lie in between 1 and 2; the function F (*V*) can be expressed as

$$F(V) = \frac{V}{\gamma} - \frac{kT}{q}\ln\left(\frac{I(V)}{AA^{*}T^{2}}\right) \quad (10)$$

where I(V) is current obtained from the I-V experimental data, γ is the dimensionless arbitrary integer greater than the value of the n obtained from ln(I)-V characteristics.

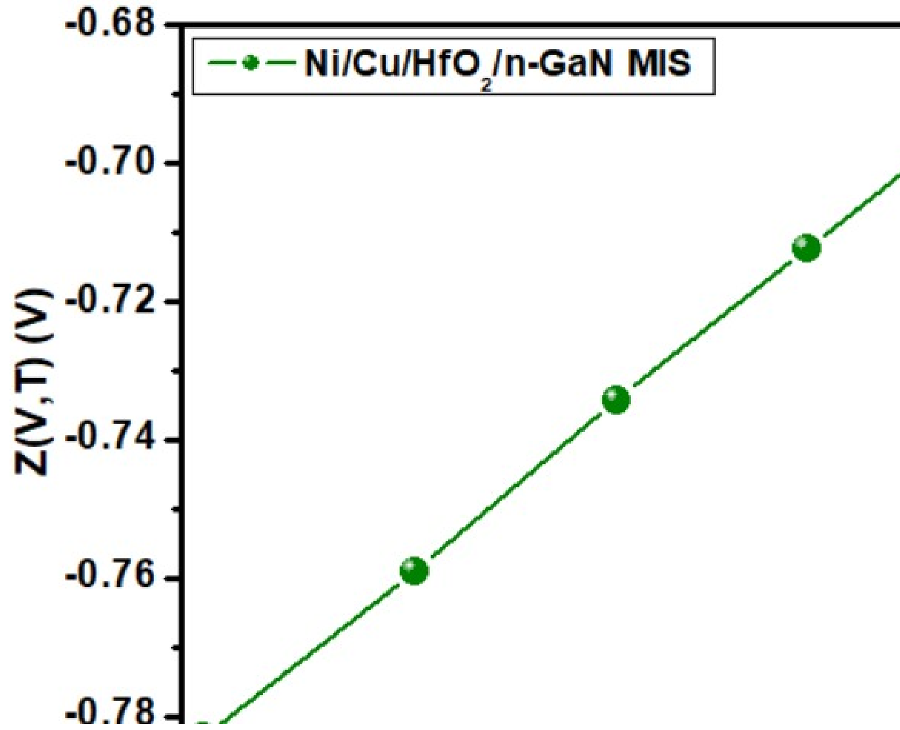

Fig. 4. Plot of Z(V,T) versus V_d for the Mo/HfO_2/n-Si MIS SD

Once the minimum of the F(V) versus V plot is determined, the value of BH can be calculated as

$$\Phi_b = F(V_0) + \frac{V_0}{\gamma} - \frac{kT}{q} \quad (11)$$

where $F(V_0)$ is the minimum point of F(V) and V_0 is the corresponding voltage. Fig. 5 shows the F(V)-V plot of the $Mo/HfO_2/n$-Si MIS diode. From Norde's function, the value of R_S value can be determined as follows

$$R_S = \frac{kT(\gamma - n)}{qI_0} \tag{12}$$

where I_0 is the corresponding current at the minimum point of $F(V_0)$. The Φ_b and R_S values are extracted from Norde plot, were found to be 0.89 eV and 2998 kΩ for MIS diode.

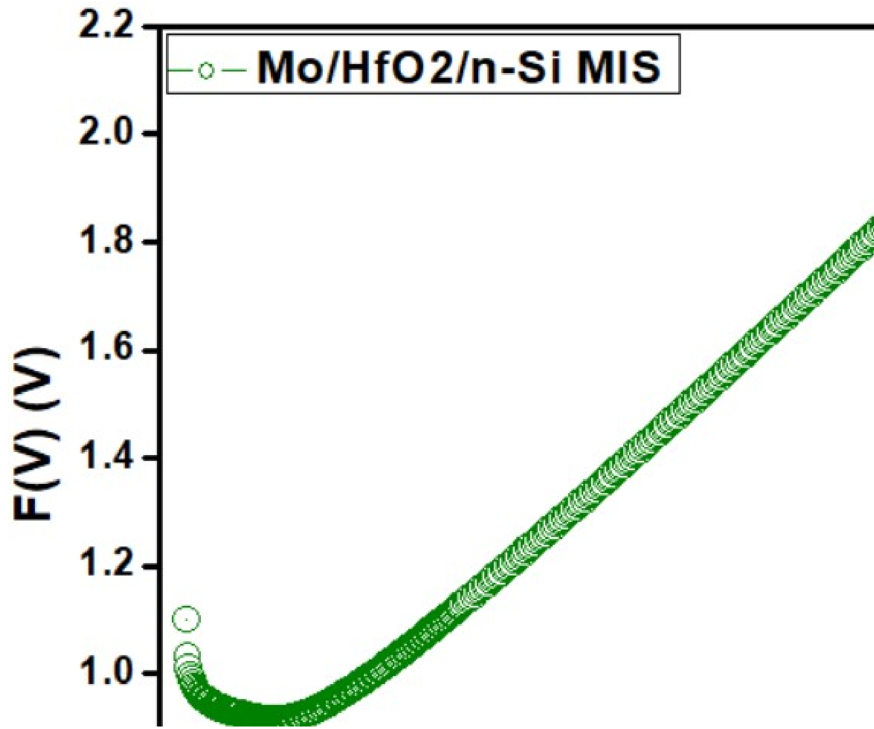

Fig. 5. The Norde plot for the $Mo/HfO_2/n$-Si MIS SD

Analysis indicates that there is slight dissimilarity in the Φ_b values derived from the forward bias ln(I)-V, Cheung's functions and Norde function, that may be attributed to the extraction from various regions of the forward bias ln(I)-V characteristics. However, the R_S values obtained from the Norde function is higher than that obtained from the Cheung's functions. Cheung's functions are only applied to the nonlinear region in high voltage section of the forward bias ln(I)-V characteristics, while Norde's function is applied to the full forward bias

region of the ln(I)-V characteristics of the diode.As a result, the approaches used here are trustworthy and efficient.

Fig.6 denotes the current transport mechanism (CTM) in the forward-bias Mo/HfO_2/n-Si MIS diode. The log (*I*) versus log (*V*) shows different linear regions (I, II, and III) yielding three different slopes. In Region-I, the calculated slope value is 1.1 which is close to unity indicating ohmic behaviour. The reason for this may be due to dopants and/or carriers which were created thermally [29].

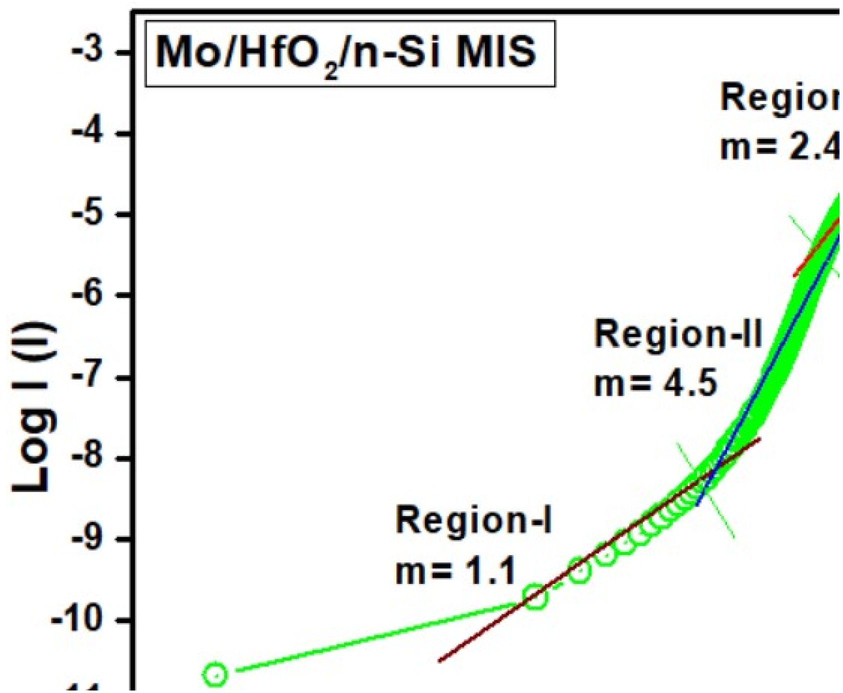

Fig. 6. The forward bias log (*I*) versus log (*V*) plot for the Mo/HfO_2/n-Si MIS diode

The slope value estimated in the region-II was 4.5 which is higher than 2 may be attributable to the space-charge-limited current (SCLC) by way of presence of isolated trapping levels in Si layer as well as in high-k HfO_2 layer. When fitting was made in region-III, the value of slope decreases to 2.4 indicating that the prepared MIS SD reaching the trap-filling limit [30-32]. This analysis leads to the conclusion that there is clear transition in the carrier transport mechanism at the interfaces of Mo/HfO_2/n-Si MIS diodeas a function of applied voltage.

To know the current conduction mechanisms that are taking place in the extracted reverse-bias *I–V* characteristics of the fabricated Mo/HfO_2/n-Si MIS diode, ln (I_R) versus $V_R^{1/2}$ plot was made and is shown in Fig. 7. This plot allows one to know whether Poole–Frenkel emission (PFE) or Schottky emission (SE) conduction mechanisms is taking place in the extracted reverse-bias *I-V* curves of the fabricated device.

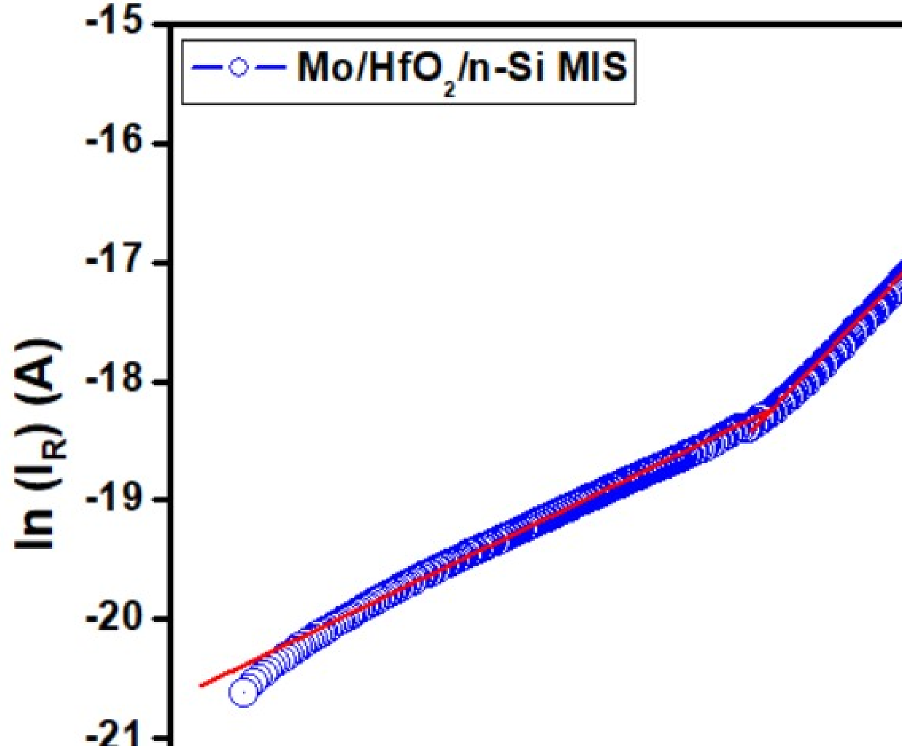

Fig. 7. Plot of ln (I_R) versus $V^{1/2}$ for the Mo/HfO_2/n-Si MIS diode

In the reverse bias, if the current is dominated by PFE mechanism which can be expressed as [33]

$$I_R = I_0 \exp\left(\frac{\beta_{PF} V^{1/2}}{kT^{\ 1/2}}\right) \quad (13)$$

For the Schottky emission (SE) mechanism is defined as

$$I_R = AA^{*}T^{2} \exp\left(-\frac{\Phi_b}{kT}\right) \exp\left(\frac{\beta_{SC} V^{1/2}}{kTd^{1/2}}\right) \quad (14)$$

where “d” is the thickness of the film, β_{PF}, and β_{SC} have the usual meanings [34]. The following expression can be used to calculate the theoretical values ofβ_{PF} and β_{SC}:

$$2\beta_{SC} = \beta_{PF} = \left(\frac{q^3}{\pi\varepsilon_0\varepsilon_r}\right)^{1/2} (15)$$

β_{PF} is always twice that of β_{SC}. However, in the case the MIS diode exhibit two distinct regions observed (Fig. 7) that show the two different conduction mechanisms that occur in the reverse bias. The extracted slope values are 5.26×10^{-5} $eVm^{1/2}V^{-1/2}$ in the lower bias region(region I) and 1.31×10^{-5} $eVm^{1/2}V^{-1/2}$ in the higher bias region (region II) for the MISSD. The extracted slope value in region I is found to be nearly matched with the theoretical value of Poole-Frenkel lowering coefficients.Hence, the reverse leakage current conduction mechanism is dominated by the Poole-Frenkel emission in region I. This indicates that the carrier transport occurs from the metal into conductive dislocations through traps states than through straight emission from the metal [35,36]. However, the extracted slope value in the region II is nearly matched with the theoretical value of Schottky lowering coefficients. This suggests that the Schottky emission is the dominant current conduction mechanism in the region II where current conduction takes place through the interface rather than from bulk material. This is due to the sub-atomic structure and non-uniformity of the dielectric layer employed here [37-40].

Conclusions

In summary, the HfO_2thin film was deposited on n-Sisemiconductor by using radio frequency (RF) magnetron deposition technique. The structural and surface morphological properties of HfO_2/n-Siinterface have been explored by XRD and XPS techniques. To study the electrical properties of fabricated Mo/HfO_2/n-Si MIS diode, I-V measurements are used at room temperature. Experimental results show that the MIS diode shows a good rectifying behavior, lower leakage current. The evaluated Φ_b of the MIS diode is very high. The enhancement of the Φ_b attributed to the fact that the HfO_2 interlayers enhances the effective Φ_b by influencing the depletion region of n-Si. Several methods have been used to extract

diode parameters, such as Φ_b, n and Rs from the experimentally obtained I-V characteristics. Steadiness in the extracted values using dissimilar methods was observed. From the forward-bias *I–V* curves of Mo/HfO_2/n-Si MIS diode, conduction mechanisms suchas ohmic is found to be active in the low-voltage regimewhereas SCLC at high voltage regimes, respectively. Furthermore,reverse *I–V* characteristics interpreted that Poole-Frenkel and Schottky emissions are the dominant current conduction mechanisms in the lower and higher bias regions. To conclude, the bettermentin rectification ratio, SBHs and good fitting ofexperimental data to equations of different methods wereascribed to the facts of deliberately deposited HfO_2andundopedGaN buffer layers in the fabricated Mo/HfO_2/n-Si MIS diode.Hence, our research results are helpful for the strategy and manufacture of high-performance n-Si-based MIS devices.

References:

[1]. Y. Atasoy, M.A. Olgar, E. Bacaksiz, J. Mater. Sci. 30, 10435–10442 (2019)

[2]. F.A. Mir, S. Rehman, K. Asokan, S.H. Khan, G.M. Bha, J. Mater. Sci. 25, 1258–1263 (2014).

[3]. H.H. Gullu, D.E. Yildiz, J. Mater. Sci. 30, 19383–19393 (2019).

[4]. J.B. Park, W.S. Lim, B.J. Park, I.H. Park, Y.W. Kim, G.Y. Yeom, J. Phys. D Appl. Phys. 42, 055202 (2009)

[5]. C. Buttay, H.-Y. Wong, B. Wang, M. Xiao, C. Dimarino, Y. Zhang, Microelectron. Reliab. 114, 113743 (2020).

[6]. G. He, L.Q. Zhu, M. Liu, Q. Fang, L.D. Zhang, Appl. Surf.Sci. 253, 3413 (2007).

[7]. S.Y. Lee, S. Chang, J.S. Lee, Thin Solid Films 518, 3030(2010)..

[8]. M.H. Al-Dharob, A. Kokce, D.A. Aldemir, A.F. Ozdemir, S. Altındal, J. Phys. Chem. Solids 144, 10952 (2020).

[9]. C. Liu, E. F. Chor, L. S. Tan, Appl. Phys. Lett. 88 (2006) 173504(1-3).

[10]. K. Cico, J. Kuzmik, D. Gregusova, R. Stoklas, T. Lalinsky, A. Georgakilas, D. Pogany, K. Frohlich, Microelectron. Reliab. 47 (2007) 790-793.

[11]. S. Kim, Y. Hori, W.-C. Ma, D. Kikuta, T. Narita, H. Iguchi, T. Uesugi, T. Kachi, T. Hashizume,Jpn. J. Appl. Phys. 51 (2012)060201(1-3).

[12]. A. Shetty, B. Roul, S. Mukundan, L. Mohan, G. Chandan, K. J. Vinoy, S. B. Krupanidhi, AIP Advances 5 (2015) 097103(1-11).

[13]. V. Manjunath, V. Rajagopal Reddy, P.R. Sekhar Reddy, V. Janardhanam, Chel-Jong Choi, Curr. Appl. Phys. 17 (2017) 980-988.

[14]. C. Venkata Prasad, M. Siva Pratap Reddy, V. Rajagopal Reddy, Chinho Park, Appl. Surf. Sci. 427 (2018) 670-677.

[15]. H.-I. Chen, C.-H. Chang, H.-H. Lu, I-P. Liu, W.-C. Chen, B.-Y. Ke, W.-C. Liu, Sens. Actuators B: Chem. 262 (2018) 852-859.

[16]. A. Vinod, M. Singh Rathore, N. SrinivasaRao, Vacuum 155,339–344 (2018).

[17]. P.R. Sekhar Reddy, V. Janardhanam, K.-H. Shim, V. Rajagopal Reddy, S.-N. Lee, S.-J. Park, C.-J. Choi, Vacuum 171, 109012 (2020).

[18]. I. Karaduman, O. Barın, M. Ozer, S. Acar, J. Electr. Mater.45, 8 (2016).

[19]. P. Harishsenthil, J. Chandrasekaran, R. Marnadu, P. Balraju,C. Mahendarn, Physica B 594, 412336 (2020).

[20]. I.R. Kaufmann, A. Pick, M.B. Pereira, H. Boudinov, Thin Solid Films 621, 184–187 (2017).

[21]. A. K. Mondal, L. K. Ping, M. A. S. M. Haniff, M. A. M. Sarjidan, B. T. Goh, M. A. Mohamed, ACS Omega 7 (2022) 2252-2259.

[22]. X. Luo, Y. Li, H. Yang, Y. Liang, K. He, W. Sun, H.-H. Lin, S. Yao, X. Lu, L. Wan, Z. Feng, Crystals 8 (2018) 248(1-16).

[23]. E. H. Rhoderick and R. H. Williams: Metal-Semiconductor Contacts, 2nd ed., (Oxford, Clarendon press, 1988) p. 33.

[24]. V. Rajagopal Reddy, V. Janardhanam, Jin-Woo Ju, Hyobong Hong, Chel-Jong Choi, Semicond. Sci. Technol. 29 (2014) 075001(6pp).

[25]. V. Rajagopal Reddy, V. Janardhanam, Jin-Woo Ju, Hyobong Hong, Chel-Jong Choi, Semicond. Sci. Technol. 29 (2014) 075001(6pp).

[26]. M. Saglam, A. Ates, B. Guzeldir, A. Astam, M.A. Yildirım, J. Alloy. Compd. 484 (2009) 570-574.

[27]. R. T. Tung, Phys. Rev. B 45 (1992) 13509-13523.

[28]. A. Kumar, M. Heilmann, M. Latzel, R. Kapoor, I. Sharma, M. Gobelt, S. H. Christiansen, V. Kumar, R. Singh, Sci. Rep. 6 (2016) 27553(1-11).

[29]. S. Kumar, M.V. Kumar, S. Krishnaveni, Semicond54, 169 (2020).

[30]. K. Ashish, V. Seema, R. Singh, J. Nano-Electron. Phys. **3**, 671 (2011).

[31]. C. Venkata Prasad, V. Rajagopal Reddy, Chel-Jong Choi, Appl. Phys. A 123 (2017) 279(1-10).

[32]. Y.S. Ocak, M. Kulakci, T. Kılıcoglu, R. Turan, K. Akkılıc, Synth. Met. **159**, 1603 (2009).

[33]. A.A. Kumar, V.R. Reddy, V. Janardhanam, H.D. Yang, H.-J. Yun, C.J. Choi, J. Alloys Compd. 549, 18 (2013).

[34]. P. R. Sekhar Reddy, V. Janardhanam, V. Rajagopal Reddy, Min Hyuk Park, · Chel-Jong Choi, Applied Physics A (2021) 127:803.

[35]. V.R. Reddy, V. Manjunath, V. Janardhanam, Y.-H. Kil, C.-J. Choi, J. Electron. Mater. 43, 3499 (2014).

[36]. K. Akkılıc, Y.S. Ocak, T. Kılıcoglu, S. Ilhan, H. Temel, Curr. Appl. Phys. 10, 337 (2010).

[37]. I. Rahim, M. Shah, M. Iqbal, F. Wahab, A. Khan, S.H. Khan, Phys. B 524, 97 (2017).

[38]. A. Tataroglu, Chin. Phys B. 22, 068402 (2013).

[39]. S. AltındalYerişkin, J Mater Sci: Mater Electron. 30 (2019).

[40]. A. Buyukbas-Ulusan, S. Altındal-Yerişkin, A. Tataroğlu, J. Mater. Sci. Mater. Electron. 29 (2018).